Molecular Characterization and Pathogenicity of Diaporthe Species Causing Nut Rot of Hazelnut in Italy

1

Molecular Characterization and Pathogenicity of *Diaporthe* Species Causing Nut Rot of Hazelnut in Italy

Muhammad Waqas[1], Vladimiro Guarnaccia[1,2], Simone Bardella[3], Davide Spadaro[1,2,†]

[1]Department of Agricultural, Forest and Food Sciences (DISAFA), University of Torino, Largo Braccini 2, 10095 Grugliasco (TO), Italy

[2]AGROINNOVA – Centre of Competence for the Innovation in the Agro-environmental Sector, University of Torino, Largo Braccini 2, 10095 Grugliasco (TO), Italy

[3]Fondazione Agrion - Via Falicetto, 24, 12030 Manta (CN), Italy

†Corresponding author: D. Spadaro; davide.spadaro@unito.it

Keywords: *Corylus avellana*; *Diaporthe eres*; hazelnut; nut rot; pathogenicity; phylogeny

Abstract

Hazelnut (*Corylus avellana*), a nut crop that is rapidly expanding worldwide, is endangered by a rot. Nut rot results in hazelnut defects. A survey was conducted in north-western Italy during 2020 and 2021 to identify the causal agents of hazelnut rots. Typical symptoms of black rot, mold, and necrotic spots were observed on hazelnut nuts. The prevalent fungi isolated from symptomatic hazelnut kernels were *Diaporthe* spp. (38%), *Botryosphaeria dothidea* (26%), *Diplodia seriata* (14%), and other fungal genera with less frequent occurrences. Among 161 isolated *Diaporthe* spp., 40 were selected for further analysis. Based on morphological characterization and multi-locus phylogenetic analysis of the ITS, *tef1*- *α*, and *tub2*, seven *Diaporthe* species were identified as *D. eres*, *D. foeniculina*, *D. novem*, *D. oncostoma*, *D. ravennica*, *D. rudis*, and *D. sojae*. *D. eres* was the main species isolated from hazelnut rots, in particular from moldy nuts. Pathogenicity test performed on hazelnut nuts 'Tonda Gentile del Piemonte' using a mycelium plug showed that all the *Diaporthe* isolates were pathogenic on their original host. To our knowledge, this work is the first report of *D. novem*, *D. oncostoma* and *D. ravennica* on hazelnut nuts worldwide. *Diaporthe foeniculina*, *D. rudis*, and *D. sojae* were reported for the first time as agents of hazelnut nut rot in Italy. Future studies should focus on the comprehension of epidemiology and climatic conditions favoring the development of *Diaporthe* spp. on hazelnut. Prevention and control measures should target *D. eres*, representing the main causal agents responsible for defects and nut rot of hazelnuts in Italy.

Introduction

Hazelnut (*Corylus avellana* L.) belongs to Betulaceae family, which is native to Europe and Western Asia, where it is widely distributed (Arciuolo et al. 2020). Hazelnut production

increased in the last several years in response to a high demand for its health benefits from fiber and nutrients (Glei et al. 2018; Nunzio 2019), but also for its massive use in spreadable creams and other confectionery products (Silvestri et al. 2021). The main producers of hazelnuts are Turkey, Italy, and the USA. In Italy, hazelnut is the major nut crop, cultivated on 84,440 ha, with an annual production of about 118,791 t (ISTAT 2022). The cultivation of hazelnut is spread all over Italy, from north to south, with main production regions as Latium (38%), Campania (37%), and Piedmont (13%) (Scarpari et al. 2020).

Hazelnut production is threatened by various fungal pathogens and disorders which reduce nut quality and yield by altering its kernel (Arciuolo et al. 2022; Battilani et al. 2018; Teviotdale et al. 2002) and can release mycotoxins (Spadaro et al. 2020; Valente et al. 2020). Several defects are reported on hazelnut kernels, such as inner discoloration, necrosis, and presence of blemishes, which reduce the market quality standards (Arciuolo et al. 2020). Hazelnut rot, called "avariato" (spoiled) in Italian, affects 3 to 7% of the nuts every year, causing significant economic losses (Vitale et al. 2020). Different fungal genera were isolated from rotten hazelnuts: *Alternaria*, *Aspergillus*, *Cladosporium*, *Colletotrichum*, *Diaporthe*, *Fusarium*, *Penicillium* *Pestalotiopsis*, and *Phoma* in the Caucasus region (Battilani et al. 2018); *Alternaria*, *Colletotrichum*, *Fusarium*, and *Phomopsis* in central Italy (Librandi et al. 2006); *Alternaria*, *Botryosphaeria*, *Cladosporium*, *Colletotrichum, Diaporthe*, *Didymella*, *Fusarium,* and *Phoma* in northern and southern Italy (Vitale et al. 2020). Among the fungal pathogens, *Diaporthe* spp. seem to play a major role in the occurrence of hazelnut defects in the Caucasus region (Arciuolo et al. 2022; Battilani et al. 2018), but it is unclear which of the above-mentioned fungal genera play a key role in Italy.

The genus *Diaporthe* (anamorph *Phomopsis*) belongs to Diaporthaceae family and was originally established with *Diaporthe eres* as the typified species isolated from *Ulmus* sp. in Germany (Nitschke 1870; Senanayake et al. 2017). The members of *Diaporthe* genus represent a cosmopolitan group of fungi which include plant pathogens, saprobes on decaying tissues and endophytes widely distributed in tropical, and temperate regions worldwide (Guarnaccia et al. 2018; Marin-Felix et al. 2019; Yang et al. 2020). *Diaporthe* spp. are causal agents of diseases on a wide range of economically important plant hosts, such as horticultural, forest, ornamentals, and fruit crops (Bertetti et al. 2018; Dissanayake et al. 2017; Guarnaccia and Crous, 2018; Huang et al. 2015; Prencipe et al. 2017; Thompson et al. 2011; Udayanga et al. 2014; Yang et al. 2018). Historically, *Diaporthe* spp. were considered monophyletic group based on unique and typical *Phomopsis* spp. asexual and sexual morphs (Gomes et al. 2013). However, paraphyletic nature was revealed by Gao et al. (2017) showing that the genera *Phaeocytostroma*, *Stenocarpella* (Lamprecht et al. 2011), *Pustulomyces* (Dai et al. 2014), *Ophiodiaporthe* (Fu et al. 2013) and *Mazzantia* (Wehmeyer 1926) are embedded in *Diaporthe s. lat.* Moreover, Senanayake et al. (2017) included *Diaporthe*-like clades within the order Diaporthales.

Pathogen identification at species level is crucial to understand the biology and epidemiology and to develop an appropriate disease management (Santos et al. 2017; Yang et al. 2018). Traditionally, *Diaporthe* species identification was based on culture characteristics, morphology, and host association (Udayanga et al. 2011; Yang et al. 2020), but morphological identification was unreliable for species identification because of high similarity of *Diaporthe* spp. (Dissanayake et al. 2017; Udayanga et al. 2011). Several studies based on the use of multi-locus phylogenetic analyses solved the boundaries within *Diaporthe* genus (Gomes et al. 2013; Marin-Felix et al. 2019; Udayanga et al. 2012). Mostly, internal transcribed spacer (ITS), translation

elongation factor-1α (*tef-1α*), beta tubulin (*β-tubulin)*, calmodulin *(CAL)*, and histone *(HIS)* genes are used for molecular characterization of *Diaporthe* spp. (Guarnaccia et al. 2018; Yang et al. 2020).

In Northern Italy, hazelnuts often show nut rot. Several fungi have been associated to nut rot in Italy (Librandi et al. 2006; Vitale et al. 2020). However, the role of the causal agents, and in particular of *Diaporthe* spp., has not been clarified. Moreover, it is unclear which species of *Diaporthe* are involved in the development of hazelnut nut rot. In order to investigate and better understand the etiology of defected kernels, a monitoring of their possible causal agents was performed between 2020 and 2021. The aims of the present study were (i) to isolate and identify the fungal species associated with hazelnut nuts defects in Northern Italy, (ii) to evaluate the genetic diversity of *Diaporthe* spp. associated with hazelnut nuts defects in Northern Italy, and (iii) to evaluate the pathogenicity of the species found.

Materials and methods

Sampling and isolation

Field surveys were conducted during November-December each in 2020 and 2021 in nine orchards located in Piedmont, Northern Italy. A total of 420 nut samples were collected from defected hazelnuts (moldy, black rotted, and necrotic) at BBCH 89 (nuts separated from the husk at the basal scar; Paradinas et al. 2022) (**Fig. 1**). Symptomatic kernels cut in half were disinfected in 1% sodium hypochlorite for 1 min, rinsed in sterile water for 1 min, and dried on sterile filter paper. Then five small pieces of half cut kernels were placed on potato dextrose agar (PDA, VWR international, Leuven, Belgium) containing streptomycin (0.025g/l). The PDA plates (9

cm diameter) were incubated at 23 ± 2 °C with a cycle of 12 h of light and 12 h of darkness for 2-3 days depending on colony growth. Pure cultures were obtained after 10 days by transferring the mycelium plug from the edge of the colonies and placed in fresh PDA plates. Isolates used in this study were maintained and kept at -80 °C in the culture collection of the University of Turin, Torino, Italy.

Macro- and micro-morphological analysis

Mycelial plugs (5 mm diameter) were taken from the margins of actively growing colonies on PDA and transferred onto the center of Petri dishes containing 2% tap water agar supplemented with sterile pine needles (PNA; Smith et al. 1996) and PDA and incubated at room temperature (22± 2 °C) under a 12-h near-ultraviolet light/12-h dark cycle to induce sporulation according to Gomes et al. (2013) and Lombard et al. (2014). Colony characters and pigment production on PDA and PNA were noted after 7 and 10 days. Colony colors were ranked according to Rayner (1970). Cultures were observed periodically for the development of ascomata and conidiomata. Morphological characteristics were examined by mounting fungal structures in clear lactic acid. Using an Eclipse 55i microscope (Nikon, Tokyo, Japan), 30 measurements at 1000× magnification were performed per isolate. Initially, identification was performed by colony and conidial morphology as described by Phillips et al. (2013), and then based on molecular identification by using internal transcribed spacer sequence amplified with primers ITS 1 and ITS 4 (White et al. 1990).

DNA extraction and PCR amplification

Forty isolates of *Diaporthe* species were selected based on morphological analysis, DNA sequence, and geographical origin data for further study (**Table S1**).

Genomic DNA was extracted from selected isolates of *Diaporthe* spp. using E.Z.N.A. Fungal DNA mini kit (Omega Bio-tek, Darmstadt, Germany) from 100 mg of mycelium grown on PDA according to the manufacturer's instructions. Partial regions of three loci were amplified. The primer sets ITS1 (5′-TCCGTAGGTGAACCTGCGG-3′)/ITS4 (5′-TCCGCTTATTGATATGC-3′) (White et al. 1990) were used to amplify the internal transcribed spacer (ITS) of ribosomal DNA. Primer pair EF1-728F (5′-CATCGAGAAGTTCGAGAAGG-3′)/EF1-986R (5′-TACTTGAAGGAACCCTTACC-3′) (Carbone and Kohn 1999) were used to amplify partial translation elongation factor 1-α gene (*tef1-α*), and the beta-tubulin (*tub2*) gene was amplified using primers Bt2a (5′ GGTAACCAAATCGGTGCTGCTTTC 3′) and Bt2b (5′ ACCCTCAGTGTAGTGACCCTTGGC 3′). In case of lack of amplification of beta-tubulin gene, T1 (5′-AACATGCGTGAGATTGTAAGT-3′) and Bt2b (5′-ACCCTCA-GTGTAGTGACCCTTGGC-3′) primers were used (Glass and Donaldson 1995; O'Donnell and Cigelnik 1997). The PCR amplification mixtures and cycling conditions for all three genes were performed according to Guarnaccia and Crous (2018). The amplification products were analyzed on 1% agarose (VWR Life Science AMRESCO® Biochemicals) after staining with GelRed™. PCR products were purified with the PCR Purification Kit (QIAquick®, Germany) before sequencing by Macrogen Europe B. V. (Amsterdam, Netherlands). The obtained sequences were analyzed and using the Geneious v. 11.1.5 program (Auckland, New Zealand).

Phylogenetic analysis

The sequences obtained from the 40 strains in this study were subjected to a blast search in NCBI's GenBank (https://blast.ncbi.nlm.nih.gov/Blast.cgi) nucleotide database to determine the closest species for a taxonomic framework of the studied isolates. The results of Blast analysis indicated that all the isolates belonged to *Diaporthe* genus. The sequences generated in this study and reference sequences of *Diaporthe* spp. (Hilário et al. 2021) were initially aligned by using the MAFFT v. 7 online servers (http://mafft.cbrc.jp/alignment/server/index.html) (Katoh and Standley 2013), and then manually adjusted in MEGA v. 7 (Kumar et al. 2016). To achieve the sub-genus identification of the *Diaporthe* spp., phylogenetic analysis was performed first individually for each gene and then as a multilocus analysis of three loci (ITS, *tef-1α* and *tub2*). The phylogeny was based on Bayesian Inference (BI) and Maximum Parsimony (MP) for the multi-locus analysis (**Fig. 2**). For BI, the best evolutionary model for each locus was determined using MrModeltest v. 2.3 (Nylander 2004) and incorporated into the analysis. MrBayes v. 3.2.5 (Ronquist et al. 2012) was used to generate phylogenetic trees under optimal criteria per partition. The Markov Chain Monte Carlo (MCMC) analysis used four chains and started from a random tree topology. The heating parameter was set at 0.2 and trees were sampled every 1,000 generations. The analysis stopped when the average standard deviation of split frequencies was below 0.01. The MP analysis was performed using Phylogenetic Analysis Using Parsimony (PAUP) v. 4.0b10 (Swofford 2003). Phylogenetic relationships were estimated by heuristic searches with 100 random addition sequences. Tree bisection-reconnection was used, with the branch swapping option set on 'best trees', with all characters equally weighted and alignment gaps treated as fifth state. Tree length (TL), consistency index (CI), retention index (RI), and rescaled consistence index (RC) were calculated for parsimony, and the bootstrap analysis (Hillis

and Bull 1993) were based on 1,000 replications. Sequences generated in this study were deposited in GenBank (**Table S2**).

Prevalence and distribution of *Diaporthe* spp.

The prevalence of *Diaporthe* spp. in hazelnut nuts collected from different sites in the investigated area was calculated according to Hilário et al. (2021). The Isolation Rate (RI) was calculated for each species using the formula:

$$RI\ \% = [NS / NI] \times 100$$

where NI was the total number of *Diaporthe* isolates collected during survey, NS was the number of isolates belonging to same species. Overall isolation rate was also determined by using the NI value that was equal total number of isolates from hazelnut nuts.

Pathogenicity trial

Pathogenicity of 40 *Diaporthe* strains was evaluated on detached ripening hazelnut nuts 'Tonda Gentile del Piemonte' (BBCH: 85; over 50% of the shells changed color) (Table S3). Nuts were surface disinfected with 1% NaClO and a piece of shell (5 mm diameter) was removed with a sterile cork borer. A mycelium plug of 5 mm in diameter was taken from seven days old PDA colony and placed with the mycelium in contact with the nuts inside each well in the shell. Each inoculation point of nut was wrapped with Parafilm to avoid dehydration. Three replicates per isolate and three nuts per replicate were tested. Nine control nuts were treated with a sterilized PDA plugs as described above and served as negative control. Inoculated nuts were placed in plastic trays and covered with plastic foil and inoculated at 22±2 °C for 30 days in a chamber, with a 12 h light/12 h dark period each day. At the end of the incubation period disease severity

was calculated by using a disease rating scale from 0 to 4 where 0= no visible symptoms, 1= <25% development of pycnidia, 2= 25-50% development of pycnidia, 3=50-75% development of pycnidia 4=≥75% development of pycnidia (**Fig. 3**).

Analysis of variance (ANOVA) was utilized for statistical analysis. The mean values were separated by Tukey HSD ($P < 0.05$) by using SPSS software (IBM SPSS Statistics v. 28.0.1.0).

Results

Fungal isolation and identification

On hazelnut nuts with defects, three types of symptoms were observed: black rot, moldy, and necrotic spots. Kernels were covered by white-grey mold and a few of them were totally rotten, wet, and almost black (**Fig. 1**). Fungi were identified based on their symptoms type, morphology (conidial morphology, colony shape, and color), and, when necessary, by using ITS sequencing.

The prevalent fungi isolated from symptomatic hazelnut kernels were *Diaporthe* spp. (38%), *Botryosphaeria dothidea* (26%), and *Diplodia seriata* (14%). Moreover, *Alternaria* spp., *Aspergillus* spp., *Fusarium* spp., Mucorales, *Neofusicoccum* spp., *Penicillium* spp., and *Trichothecium roseum* were isolated from nuts but with incidence lower than 6%. *Diaporthe* spp. were isolated from moldy nuts (68%), followed by necrotic nuts (17%) and black rotted nuts (15%). Members of Botryosphaeriaceae and *Alternaria* spp. were isolated only from black rotted and necrotic nuts. Whilst *Fusarium* spp. and *Trichothecium roseum* were isolated only from moldy nuts. Other fungal pathogens were isolated from mixed nuts (moldy, necrotic or black rotted).

Diaporthe spp. were isolated from all locations with different frequency: Lu and Cuccaro (30%), Murazzano (82%), Marsaglia (64%), Rodello (47%), Belvedere Langhe (32%), Cravanzana (36%), Cortemilia (50%), Borgo D'Ale (8%), and Cavaglià (42%) (**Table 1**).

Phylogenetic analysis

To further explore the diversity of the *Diaporthe* spp. isolates and to assign the species, three genes were sequenced: ITS, *tub2*, and *tef-1α.* A combined alignment of the three loci was analyzed. The combined alignment consisted of 111 sequences including the outgroup *Diaporthella corylina* (CBS 121124). The final dataset comprised of 1,362 nucleotides (ITS: 1-473, *tub2*: 480-876, *tef-1α*: 883-1,362). A total of 559 nucleotides were parsimony-informative, 194 were variable and parsimony-uninformative, and 597 were constant. A maximum of 1,000 equally MP trees were saved (Tree length = 3049, CI = 0.471, RI = 0.872, and RC = 0.410). Bootstrap support values from the MP analysis are included on the Bayesian tree in **Fig. 2**. For the BI, MrModeltest suggested that all partitions should be analyzed with Dirichlet state frequency distributions. The following models were recommended by MrModeltest and used: GTR+I+G for ITS and *tef-1α*, and HKY+G for *tub2*. In the BI, the ITS partition had 179 unique site patterns, the *tef-1α* partition had 350 unique site patterns, the *tub2* partition had 259 unique site patterns and the analysis ran for 3,495,000 generations, resulting in 3,496 trees of which 2,622 trees were samples to calculate the posterior probabilities. Multi-locus phylogenetic analysis of 40 isolates showed that 28 isolates clustered with *D. eres*, 3 isolates clustered with *D. novem*, 3 with *D. foeniculina*, and 3 with *D. rudis*. Hm-20a-2, HBr-9b-1 and HM-30-2 formed distinct lineage with *D. oncostoma*, *D. ravennica*, and *D. sojae,* respectively.

Morphology

Morphological observations from edges of the Petri dishes, supported by phylogenetic inference, were used to describe the seven species of *Diaporthe* spp. (**Fig. 4 A-I**).

Colonies of *Diaporthe sojae* growing on PDA reached 90 mm within 10 days at 25-26 °C. Colonies were white, with fluffy aerial mycelium. Reverse colonies were creamy and later developed a yellowish pigmentation in center of the Petri dish. Alpha-conidia were hyaline, aseptate, abundant, smooth, ellipsoidal and biguttulate with dimensions 5.8-7.3x2-3.2 µm mean ± SD = 6.67±0.78x2.57±0.60 (**Fig. S1 A-B; Fig. S2 A**).

Ten days colonies of *Diaporthe foeniculina* growing on PDA reached 90 mm at 25-26 °C. Colonies were white with fluffy aerial mycelium. Reverse colonies had green to yellowish pigmentation. Alpha conidia were hyaline, aseptate, smooth, ellipsoidal or fusiform, with one or many guttules with dimensions 7.6-9.5x2.5-2.9 µm mean ± SD = 8.6±0.96x2.7±0.21 (**Fig. S1 C.D; Fig. S2 B**).

Diaporthe novem had ten-day colonies on PDA reaching 90 mm at 25-26 °C. Colonies were flat, fluffy, and white to greyish colonies in center with white aerial mycelium at the margins of the Petri dish. Colony reverse had black circles and white margins. Alpha-conidia were hyaline, unicellular, oval to cylindrical, biguttulate with obtuse ends, with dimensions of 6.9-9.1x2.5-2.9 µm, mean ± SD =8.1±1.11x2.73±0.21 µm (**Fig. S1 E-F; Fig. S2 C**).

Ten days colonies of *Diaporthe ravennica* growing on PDA reached 90 mm at 25-26 °C. Colonies were white, spreading to the edge in wavy appearance, with pycnidia production in middle of plate, medium flat or dense. Reverse colony was creamy, radiating white outwardly with black dots in middle. Alpha-conidia were smooth, hyaline, aseptate, multi-guttulate, ovate

to ellipsoidal with dimensions 8.3-11.9x2.5-4.3 µm mean ± SD =10.1±1.80x3.30±0.92 (**Fig. S1 G-H; Fig. S2 D**).

Colonies of *Diaporthe rudis* growing on PDA reached 85 mm within 4 weeks at 25-26 °C. Colonies were white and turn brown gradually, fluffy, and flat, radiating outwardly to the edge, with brown mycelium. Colony reverse was greyish with brown halos. Alpha conidia were ellipsoidal, hyaline, biguttulate and smooth. Dimensions of conidia were 7.5-8.5x2.4-2.7 µm mean ± SD =7.97±0.50x2.57±0.15 µm (**Fig. S1 I-J; Fig. S2 E**).

Colonies of *Diaporthe eres* were white greyish, fluffy aerial mycelium with abundant pycnidia at maturity. Colony reverse had dark pigmentation in center and whitish from edges of the Petri dish. Colonies growing on PDA reached 90 mm at 25-26 °C after 10 days. Alpha conidia were ovate to ellipsoidal, aseptate, smooth, hyaline, biguttulate, and base subtruncate with dimensions of 8.5-11.1x 3.5-4.5 µm, mean ± SD =9.7±1.31x3.67±0.76 (**Fig. S1 K-L; Fig. S2 F**).

Colonies of *Diaporthe oncostoma* were smooth and flat with no exudate. Dense fluffy mycelium was observed. Colony reverse had yellowish green and periphery umber. Colonies growing on PDA reached 25 mm at 25-26 °C after 10 days. Alpha conidia were hyaline, septate, and bent cylindrical with dimensions of 11-14.5x 3.2-4.9 µm, mean ± SD = 12.83±1.76x4.20±0.89 (**Fig. S1 M-N; Fig. S2 G**).

Prevalence and distribution of *Diaporthe* spp.

Diaporthe spp. were isolated from all the sites surveyed (Lu and Cuccaro, Murazzano, Marsaglia, Rodello, Belvedere Langhe, Cravanzana, Cortemilia, Borgo D'Ale, and Cavaglià) showing symptoms of black rot, moldy, and necrosis. In particular, *Diaporthe* spp. were predominantly isolated from moldy nuts. Based on morphology, among 161 *Diaporthe* spp.

isolates, *D. eres* was the dominant species, representing 92.5 % of the isolates collected. Three strains per species of *D. rudis*, *D. novem*, and *D. foeniculina* were isolated. Only one isolate was found per each of the species *Diaporthe oncostoma*, *D. sojae*, and *D. ravennica*.

Diaporthe eres was predominantly isolated in all the geographical areas: it was the only species isolated in Belvedere Langhe, Cravanzana, Cortemilia, and Borgo D'Ale. Moreover, it represented the most isolated species in the other geographical areas: 94 %, 88 %, 93 %, 88 %, and 86% of the collected isolates were *D. eres* in Lu and Cuccaro, Murazzano, Marsaglia, Rodello, and Cavaglià, respectively. Whilst *D. rudis* and *D. novem* were recovered only from three and two towns, respectively, with an abundance lower than 15 % (**Fig. 5**).

Pathogenicity test

After fifteen days, all the *Diaporthe* isolates developed lesions on the surface of inoculated kernels. Moreover, the inoculated kernels showed abundant development of pycnidia with different disease severity (disease rating scale 0-4) on the whole nut as shown in **Fig. 3 and Table S3**. In few cases internal black discoloration was also observed on nuts along with necrotic spots of variable sizes. All the *Diaporthe* isolates were successfully reisolated from all the inoculated nuts, fulfilling Koch's postulates. Control hazelnut kernels showed no internal or external symptoms.

Discussion

Hazelnut kernel defects are a serious threat for hazelnut yield, quality, and market value. The present study aimed to investigate the causal agents and the diversity of fungal species associated with rotten hazelnut nuts in Italy. During the survey performed from 2020 to 2021 in northern

Italy, we isolated and identified *Alternaria* spp., *Aspergillus*, *B. dothidea*, *Diaporthe* spp., *D. seriata*, *Fusarium* spp., Mucorales, *Neofusicoccum* spp., *Penicillium* spp., and *T. roseum* based on morphological and ITS analysis. Distinct taxonomic groups were isolated from different categories of symptoms. Members of Botryosphaeriaceae and *Alternaria* spp. were isolated only from black rotted and necrotic nuts. Whilst *Fusarium* spp. and *Trichothecium roseum* were isolated only from moldy nuts. Previously, *N. parvum* (Waqas et al. 2022), *Alternaria* spp. (Battilani et al. 2018; Belisario et al. 2004), *B. dothidea* and *D. seriata* (Luna et al. 2022) were isolated from rotten hazelnuts or other nut crops.

Diaporthe spp. were the most dominant fungi isolated from defected hazelnut nuts in northern Italy. Most *Diaporthe* spp. were isolated from moldy nuts (68%), but also from necrotic and black rotted nuts. The prevalence of *Diaporthe* spp. associated with nut rot is closely correlated to the sampling area and to the type of nut symptoms. The highest diversity of *Diaporthe* spp. was observed in Murazzano, where 51% nuts were moldy which is in agreement with previous studies on hazelnuts from Georgia and Turkey (Battilani et al. 2018; Arciuolo et al. 2020). *Diaporthe* spp. have a wide host range (Gomes et al. 2013; Lombard et al. 2014; Udayanga et al. 2015; Yang et al. 2021) and were previously reported as causal agents of diseases of hazelnut nuts (Arciuolo et al. 2020; Bai et al. 2022; Battilani et al. 2018; Gao et al. 2021; Guerrero et al. 2020) and other nut crops (Eichmeier et al. 2020; Lawrence et al. 2015; León et al. 2020; Yang et al. 2018). Previously, *Diaporthe* spp. were isolated from hazelnut nuts and identified at genus level in Italy (Vitale et al. 2020).

ITS sequence is commonly used for species identification of Diaporthaceae and Botryosphaeriaceae (Hyde et al. 2014; Marin-Felix et al. 2019). However, ITS sequence is not informative to distinguish the *Diaporthe* species because of greater intraspecific variation in ITS

332 locus as compared to interspecific variation (Chaisiri et al. 2021; Santos et al. 2010). Therefore, a
333 multi-locus phylogenetic analyses approach is used for accurate identification and resolution of
334 *Diaporthe* species (Guarnaccia et al. 2020; Lesuthu et al. 2019; Santos et al. 2017; Zapata et al.
335 2020). DNA sequence data combined with morphology has been extensively used to establish
336 the species boundaries in *Diaporthe* genus (Gao et al. 2017; Hilario et al. 2021).
337 Seven *Diaporthe* spp. were identified in this study based on morphological features and three
338 genomic regions ITS, *tef-1α* and *tub2*. The closest taxa of the seven *Diaporthe* spp. recovered in
339 this study were included in the analysis, based on BLASTn search in NCBI's GenBank
340 (https://blast.ncbi.nlm.nih.gov/Blast.cgi) nucleotide database. The final multilocus phylogenetic
341 tree differentiated *D. eres*, *D. foeniculina*, *D. novem*, *D. oncostoma*, *D. ravennica*, *D. rudis*, and
342 *D. sojae* on hazelnut nuts.
343 *D. eres* was the most frequently isolated species associated with defected hazelnut nuts from all
344 the areas of northern Italy. *D. eres* is an important plant pathogen which can infect various hosts
345 (Bai et al. 2022) and has been considered the main causal agent of hazelnut nuts defects in the
346 Caucasus region (Arciuolo et al. 2020; Battilani et al. 2018). Although *D. eres* was reported on
347 hazelnut nuts in Italy and Turkey by Arciuolo et al. (2020), most isolates could not be classified
348 at species level due to the poorly supported or non-monophyletic clade. Moreover, pathogenicity
349 of *D. eres* isolates was unknown on hazelnut nuts. However, our analysis based on three loci,
350 combined with morphological observations, clearly identified *D. eres* at species level.
351 Previously, *D. eres* was associated with hazelnut canker in China and the USA (Bai et al., 2022;
352 Gao et al., 2021; Wiman et al. 2019), and on other hosts (Guarnaccia et al. 2018; Hilário et al.
353 2021; Lombard et al. 2014; Udayanga et al. 2014; Wang et al. 2021).

Previous studies showed that *D. foeniculina* and *D. rudis* could be pathogenic or saprophytic on different host plants (Gajanayake et al. 2020; Marin-Felix et al. 2019; Udayanga et al. 2014). Recently, Guerrero et al. (2020) described *D. foeniculina* associated with black tip and necrotic spots on hazelnut kernel in Chile and stem and shoot cankers on sweet chestnuts in Italy (Annesi et al. 2016). Moreover, kernel mold of hazelnut was caused also by *D. rudis* in the USA (Pscheidt et al. 2019) and on other hosts in Italy (Dissanayake et al. 2017; Guarnaccia et al. 2020). Similarly, we detected these species associated with nut rot of hazelnut nuts in Italy. Moreover, *D. sojae* was isolated and identified for the first time from infected nuts of hazelnut in Italy, where it was already reported on hazelnut in Turkey (Arciuolo et al. 2020) and on *Glycine soja* in Italy (Gomes et al. 2013). There are no previous records of *D. novem*, *D. ravennica,* and *D. oncostoma* on hazelnut nuts. So, this study suggests that hazelnut could be a host for *D. novem*, *D. ravennica,* and *D. oncostoma.* Previously, *D. novem* was reported on *Citrus* spp. in Italy (Guarnaccia and Crous 2017) and on almond in the USA (Lawrence et al. 2015), whilst *D. ravennica* and *D. oncostoma* were reported on *Salvia* sp. and *Tamarix* sp. in Italy (Dissanayake et al. 2017; Thambugala et al. 2017) and *Robinia pseudoacacia* by Gomes et al. (2013) respectively.

In our phylogeny, the three loci used in this study were unable, when considered singularly, to discriminate *D. revennica* from *D. foeniculina*, and *D. baccae*. Separation of *D. ravennica* from *D. foeniculina*, and *D. baccae* was possible only with a combined analysis of ITS, *tef-1α*, and *tub2* regions as reported in previous studies (Aiello et al. 2022; Gajanayake et al. 2020; Phukhamsakda et al. 2020). *D. sojae* strain also formed a well-supported clade with CBS 139282 (Udayanga et al. 2015). Our results of phylogeny showed a large diversity of *Diaporthe* spp. comprising several clades and species, associated with nut rot of hazelnut nuts in Italy.

The pathogenicity tests showed that all the studied isolates were pathogenic on hazelnut nuts, resulting in different disease severity. A total of 40 strains of *Diaporthe*, belonging to *D. eres*, *D. foeniculina*, *D. novem*, *D. oncostoma*, *D. ravennica*, *D. rudis*, and *D. sojae* were able to cause nut rot of hazelnut. *D. eres* was the most virulent species as compared to the other species of *Diaporthe* which is in agreement with previous studies (Arciuolo et al. 2020; Bai et al., 2022; Battilani et al. 2018; Gao et al., 2021). Whereas *D. oncostoma* was comparatively less pathogenic (smaller lesions), suggesting that *D. oncostoma* is probably a weak pathogen on hazelnut nuts. The other species were moderately pathogenic on their original host.

In conclusion, this study elucidates the species of *Diaporthe* associated with defected hazelnut nuts in northern Italy, by using morphology analysis, molecular data, and pathogenicity. This is the first report worldwide about nut rot of hazelnut caused by *D. novem, D. oncostoma*, and *D. ravennica*, and the first report of *D. foeniculina*, *D. rudis*, and *D. sojae* as agents of nut rot of hazelnut in Italy.

In this study, we also observed the co-occurrence of *Diaporthe* spp. in the same nuts with members of Botryosphaeriaceae, as previously reported (Elfar et al. 2013; Guarnaccia et al. 2016; Moral et al. 2017). Such co-existence is not new, as it has been previously described on branch cankers and stem-end rot of different hosts in Italy and on hazelnut nuts in Caucasus region (Battilani et al. 2018; Guarnaccia et al. 2016; 2020). Furthermore, *Diaporthe* spp. are cosmopolitan fungi and can infect a range of cultivated crops and natural ecosystem as a plant pathogens or saprophytes. Taking all of this into consideration, it deserves further investigation that *Diaporthe* spp. with other members of Botryosphaeriaceae, may contribute to cause fungal trunk disease (FTD) of hazelnuts in Italy, that could be a threat to European hazelnut production.

Future studies should also focus on elucidating the epidemiology of this disease and on the environmental conditions favoring the development of *Diaporthe* spp. on hazelnut. Prevention and control measures should target *D. eres*, which showed to be the main responsible species of defects on hazelnuts in Italy.

References

Aiello, D., Guarnaccia, V., Costanzo, M. B., Leonardi, G. R., Epifani, F., Perrone, G., and Polizzi, G. 2022. Woody Canker and Shoot Blight Caused by Botryosphaeriaceae and Diaporthaceae on Mango and Litchi in Italy. Horticulturae 8:330.

Annesi, T., Luongo, L., Vitale, S., Galli, M., and Belisario, A. 2016. Characterization and pathogenicity of Phomopsis theicola anamorph of *Diaporthe foeniculina* causing stem and shoot cankers on sweet chestnut in Italy. J. Phytopathol. 164: 412–416.

Arciuolo, R., Chiusa, G., Castello, G., Camardo Leggieri, M., Spigolon, N., and Battilani, P. 2022. *Diaporthe* spp. is confirmed as the main fungus associated with defective Turkish hazelnuts. Plant Health Prog. https://doi.org/10.1094/PHP-01-22-0006-RS

Arciuolo, R., Santos, C., Soares, C., Castello, G., Spigolon, N., Chiusa, G., Lima, N., and Battilani, P. 2020. Molecular characterization of *Diaporthe* species associated with hazelnut defects. Front. Plant Sci. 11:611655.

Bai, Y., Pan, M., Gao, H., Lin, L., Tian, C., and Fan, X. 2022. Studies of *Diaporthe* Species Causing Hazelnut Canker Disease in Beijing, China, with Two New Species Described. Plant Pathol. 00:1-12.

Battilani, P., Chiusa, G., Arciuolo, R., Somenzi, M., Fontana, M., Castello, G., and Spigolon, N. 2018. *Diaporthe* as the main cause of hazelnut defects in the Caucasus region. Phytopathol. Mediterr., 57:320-333.

Belisario, A., Maccaroni, M., Coramusi, A., Corazza, L., Pryor, B. M., and Figuli, P. 2004. First report of *Alternaria* species groups involved in disease complexes of hazelnut and walnut fruit. Plant Dis. 88:426-426.

Bertetti D., Guarnaccia V., Spadaro D., Gullino M.L. 2018. First Report of Fruit Rot in European Pear Caused by *Diaporthe eres* in Italy. Plant Dis. 102:2651.

Carbone, I., and Kohn, L. M. 1999. A method for designing primer sets for speciation studies in filamentous ascomycetes. Mycologia 91:553–556.

Chaisiri, C., Liu, X., Lin, Y., Fu, Y., Zhu, F., and Luo, C. 2021. Phylogenetic and haplotype network analyses of *Diaporthe eres* species in China based on sequences of multiple loci. Biology 10:179.

Dai, D. Q., Wijayawardene N. N., Bhat, D. J., Chukeatirote, E., Bahkali, A. H., Zhao, R. L, Xu, J. C., and Hyde, K. D. 2014. *Pustulomyces* gen. nov. accommodated in Diaporthaceae, Diaporthales, as revealed by morphology and molecular analyses. Cryptogam. Mycol. 35:63-72.

Díaz, G. A., Latorre, B. A., Lolas, M., Ferrada, E., Naranjo, P., and Zoffoli, J. P. 2017. Identification and characterization of *Diaporthe ambigua*, *D. australafricana*, *D. novem*, and *D. rudis* causing a postharvest fruit rot in kiwifruit. Plant Dis. 101:1402-1410.

Dissanayake, A. J., Camporesi, E., Hyde, K. D., Wei, Z., Yan, J. Y., and Li, X. H. 2017 Molecular phylogenetic analysis reveals seven new *Diaporthe* species from Italy. Mycosphere 8:853–877.

443 Eichmeier, A., Pecenka, J., Spetik, M., Necas, T., Ondrasek, I., Armengol, J., León, M.,
444 Berlanas, C. and Gramaje, D. 2020. Fungal trunk pathogens associated with *Juglans*
445 *regia* in the Czech Republic. Plant dis.104:761-771.
446 Elfar, K., Torres, R., Diaz, G. A., and Latorre, B. A. 2013. Characterization of *Diaporthe*
447 *australafricana* and *Diaporthe* spp. associated with stem canker of blueberry in Chile.
448 Plant Dis. 97:1042-1050.
449 Fu, C. H., Hsieh, H. M., Chen, C. Y., Chang, T. T., Huang, Y. M., Ju, Y. M. 2013.
450 *OphioDiaporthe cyatheae* gen. et sp. nov., a diaporthalean pathogen causing a
451 devastating wilt disease of Cyathea lepifera in Taiwan. Mycologia 105: 861-872.
452 Gajanayake, A. J., Abeywickrama, P. D., Jayawardena, R. S., Camporesi, E., and Bundhun, D.
453 2020. Pathogenic *Diaporthe* from Italy and the first report of *D. foeniculina* associated
454 with *Chenopodium* sp. Plant Pathol. Quar. 10:172-197.
455 Gao, Y. H., Liu, F., Duan, W., Crous, P. W., and Cai, L. 2017. *Diaporthe* is paraphyletic. IMA
456 fungus 8:153-187.
457 Gao, H., Pan, M., Tian, C., and Fan, X. 2021. *Cytospora* and *Diaporthe* species associated with
458 hazelnut canker and dieback in Beijing, China. Front. cell. infect. 11.
459 Glass, N. L., Donaldson, G. C. 1995. Development of primer sets designed for use with the PCR
460 to amplify conserved genes from filamentous Ascomycetes. Appl. Environ. Microbiol.
461 61:1323–1330.
462 Glei, M., Fischer, S., Lamberty, J., Ludwig, D., Lorkowski, S., and Schlörmann, W. 2018.
463 Chemopreventive Potential of In Vitro Fermented Raw and Roasted Hazelnuts in LT97
464 Colon Adenoma Cells. Anticancer Res. 38:83-93.

Gomes, R. R., Glienke, C., Videira, S. I. R., Lombard, L., Groenewald, J. Z., and Crous, P. W. 2013. *Diaporthe*: a genus of endophytic, saprobic and plant pathogenic fungi. Persoonia: Molecular Phylogeny and Evolution of Fungi 31:1-41.

Guarnaccia, V., Martino, I., Tabone, G., Brondino, L., and Gullino, M. L. 2020. Fungal pathogens associated with stem blight and dieback of blueberry in northern Italy. Phytopathol. Mediterr. 59:229-245.

Guarnaccia, V., Groenewald, J. Z., Woodhall, J., Armengol, J., Cinelli, T., Eichmeier, A., Ezra, D., Fontaine, F., Gramaje, D., Gutierrez-Aguirregabiria, A., Kaliterna, J., Kiss, L., Larignon, P., Luque, J., Mugnai, L., Naor, V., Raposo, R., Sándor, E., Váczy, K.Z., and Crous, P. W. 2018. *Diaporthe* diversity and pathogenicity revealed from a broad survey of grapevine diseases in Europe. Persoonia: Molecular Phylogeny and Evolution of Fungi 40:135-153.

Guarnaccia, V., and Crous, P. W. 2018. Species of *Diaporthe* on Camellia and Citrus in the Azores Islands. Phytopathol. Mediterr. 57:307-319.

Guarnaccia, V., Vitale, A., Cirvilleri, G., Aiello, D., Susca, A., Epifani, F., Perrone, G. and Polizzi, G. 2016. Characterization and pathogenicity of fungal species associated with branch cankers and stem-end rot of avocado in Italy. Eur. J. Plant Pathol. 146:963-976.

Guerrero Contreras, J., Galdames Gutierrez, R., Ogass Contreras, K., Pe´rez Fuentealba, S. 2020. First report of *Diaporthe foeniculina* causing black tip and necrotic spot on hazelnut kernel in Chile. Plant dis. 104:975.

Hilário, S., Gonçalves, M. F., and Alves, A. 2021. Using genealogical concordance and coalescent-based species delimitation to assess species boundaries in the *Diaporthe eres* complex. Journal of Fungi 7:507.

488 Huang, F., Udayanga, D., Wang, X., Hou, X., Mei, X., Fu, Y., Hyde, K.D. and Li, H. 2015.
489 Endophytic Diaporthe associated with Citrus: A phylogenetic reassessment with seven
490 new species from China. Fungal Biol. 119:331-347.
491 Hyde, K. D., Dong, Y., Phookamsak, R., Jeewon, R., Bhat, D. J., Jones, E. B., Liu, N. G.,
492 Abeywickrama, P. D., Mapook, A., Wei, D., and Perera, R. H. 2020. Fungal diversity
493 notes 115–1276: taxonomic and phylogenetic contributions on genera and species of
494 fungal taxa. Fungal Diversity 100:5-277.
495 Hillis, D. M., and Bull, J. J., 1993. An empirical test of bootstrapping as a method for assessing
496 confidence in phylogenetic analysis. Systematic Biology 42:182-192.
497 ISTAT. 2021. http://dati.istat.it/Index.aspx?QueryId=33702. Accessed 13 September 2022.
498 Katoh, K., and Standley, D. M. 2013. MAFFT Multiple sequence alignment software version 7:
499 Improvements in performance and usability. Mol. Biol. Evol. 30:772-780.
500 Kumar, S., Stecher, G., and Tamura, K. 2016. MEGA7: Molecular Evolutionary Genetics
501 Analysis version 7.0 for bigger datasets. Mol. Biol. Evol. 33:1870-1874.
502 Lamprecht, S. C., Crous, P. W., Groenewald, J. Z., Tewoldemedhin, Y. T., Marasas, W. F. O.,
503 2011. Diaporthaceae associated with root and crown rot of maize. IMA Fungus 2:13-24.
504 Lawrence, D. P., Travadon, R., and Baumgartner, K. 2015. Diversity of *Diaporthe* species
505 associated with wood cankers of fruit and nut crops in northern California. Mycologia
506 107: 926-940.
507 León, M., Berbegal, M., Rodríguez-Reina, J. M., Elena, G., Abad-Campos, P., Ramón-Albalat,
508 A., Olmo, D., Vicent, A., Luque, J., Miarnau, X. and Agustí-Brisach, C. 2020.
509 Identification and characterization of *Diaporthe* spp. associated with twig cankers and
510 shoot blight of almonds in Spain. Agronomy 10:1062.

511 Lesuthu, P., Mostert, L., Spies, C. F. J., Moyo, P., Regnier, T., and Halleen, F. 2019. *Diaporthe*
512 *nebulae* sp. nov. and first report of *D. cynaroidis*, *D. novem*, and *D. serafiniae* on
513 grapevines in South Africa. Plant Dis. 103:808-817.
514 Librandi, I., Galli M., and Belisario, A. 2006. Le patologie del frutto del nocciolo in Italia, con
515 particolare riguardo alla zona del viterbese. Petria 16:125–134.
516 Linaldeddu, B. T., Deidda, A., Scanu, B., Franceschini, A., Alves, A., Abdollahzadeh, J., and
517 Phillips, A. J. L. 2016. Phylogeny, morphology and pathogenicity of Botryosphaeriaceae,
518 Diatrypaceae and Gnomoniaceae associated with branch diseases of hazelnut in Sardinia
519 (Italy). Eur. J. Plant Pathol. 146:259-279.
520 Lombard, L., van Leeuwen, G., Guarnaccia, V., Polizzi, G., van Rijswick, P., Rosendahl, K.,
521 Gabler, J. and Crous, P. 2014. *Diaporthe* species associated with Vaccinium, with
522 specific reference to Europe. Phytopathol. Mediterr. 53:287-299.
523 Luna, I. J., Besoain, X., Saa, S., Peach-Fine, E., Morales, F. C., Riquelme, N., Larach, A.,
524 Morales, J., Ezcurra, E., Ashworth, V. E. and Rolshausen, P. E. 2022. Identity and
525 pathogenicity of Botryosphaeriaceae and Diaporthaceae from *Juglans regia* in Chile.
526 Phytopathol. Mediterr. 61:79-94.
527 Marin-Felix, Y., Hernández-Restrepo, M., Wingfeld, M. J., Akulov, A., Carnegie, A. J.,
528 Cheewangkoon, R., Gramaje, D., Groenewald, J. Z., Guarnaccia, V., Halleen, F.,
529 Lombard, L., Luangsaard, J., Marincowitz, S., Moslemi, A., Mostert, L., Quaedvlieg, W.,
530 Schumacher, R. K., Spies, C. F. J., Tangavel, R., Taylor, P. W. J., Wilson, A. M.,
531 Wingfeld, B. D., Wood, A. R., and Crous, P. W. 2019. Genera of phytopathogenic fungi:
532 GOPHY 2. Stud. Mycol. 92:47-133.

Moral, J., Agustí-Brisach, C., Pérez-Rodríguez, M., Xavier, C., Raya, M. C., Rhouma, A., and Trapero, A. 2017. Identification of fungal species associated with branch dieback of olive and resistance of table cultivars to *Neofusicoccum mediterraneum* and *Botryosphaeria dothidea*. Plant Dis. 101:306-316.

Nitschke, T. 1870. *Pyrenomycetes Germanici*. 2:245 Breslau. Eduard Trewendt, Germany**.**

Nunzio, M. D. 2019. Hazelnuts as source of bioactive compounds and health value underestimated food. Curr. Res. Nutr. Food Sci. 7:17-28.

Nylander, J. A. A. 2004. MrModeltest v2. Program distributed by the author. Evolutionary Biology Centre, Uppsala University, Uppsala.

O'Donnell, K., and Cigelnik, E. 1997. Two divergent intragenomic rDNA ITS2 types within a monophyletic lineage of the fungus *Fusarium* are nonorthologous. Mol. Phylogenet. Evol. 7:103-116.

Paradinas, A., Ramade, L., Mulot-Greffeuille, C., Hamidi, R., Thomas, M. Toillon, J. 2022. Phenological growth stages of 'Barcelona' hazelnut (*Corylus avellana* L.) described using an extended BBCH scale. Sci. Hortic. 296:110902.

Phukhamsakda, C., McKenzie, E. H., Phillips, A. J., Gareth Jones, E. B., Jayarama Bhat, D., Stadler, M., ... and Hyde, K. D. 2020. Microfungi associated with Clematis (Ranunculaceae) with an integrated approach to delimiting species boundaries. Fungal diversity 102:1-203.

Prencipe, S., Nari, L., Vittone, G., Spadaro, D. (2017) First Report of *Diaporthe eres* causing stem canker on peach (*Prunus persica*) in Italy. Plant Dis. 101:1052.

554 Pscheidt, J. W., Heckert, S., Wiseman, M., and Jones, L. 2019. Fungi associated with and
555 influence of moisture on development of kernel mold of hazelnut. Plant Dis. 103:922-
556 928.
557 Rayner, R. W. 1970. A mycological colour chart. Commonwealth Mycological Institute, Kew.
558 Ronquist, F., Teslenko, M., van der Mark, P.; Ayres, D.L.; Darling, A.; Höhna, S.; Larget, B.;
559 Liu, L.; Suchard, M. A., Huelsenbeck, J. P. 2012. MrBayes 3.2: Efficient Bayesian
560 phylogenetic inference and model choice across a large model space. Syst. Biol. 61:539-
561 542.
562 Santos, L., Alves, A., Alves, R. 2017. Evaluating multi-locus phylogenies for species boundaries
563 determination in the genus Diaporthe. PeerJ, 5:e3120.
564 Santos, J. M., Correia, V. G., and Phillips, A. J. 2010. Primers for mating-type diagnosis in
565 *Diaporthe* and Phomopsis: their use in teleomorph induction in vitro and biological
566 species definition. Fungal Biol. 114:255-270.
567 Scarpari, M., Vitale, S., Di Giambattista, G., Luongo, L., De Gregorio, T., Schreiber, G., ... and
568 Voglmayr, H. 2020. *Didymella corylicola* sp. nov., a new fungus associated with hazelnut
569 fruit development in Italy. Mycol. Prog. 19:317-328.
570 Senanayake, I. C. Crous, P. W. Groenewald, J. Z. Maharachchikumbura, S. S. N. Jeewon, R.
571 Phillips, A. J. L. Bhat, J. D. Perera, R. H. Li, Q. R. Li, W. J., ... and Hyde, K. D. 2017.
572 Families of Diaporthales based on morphological and phylogenetic evidence. Stud.
573 Mycol. 86:217-296.
574 Silvestri, C., Bacchetta, L., Bellincontro, A., and Cristofori, V. 2021. Advances in cultivar
575 choice, hazelnut orchard management, and nut storage to enhance product quality and
576 safety: an overview. J. Sci. Food Agric. 101:27-43.

577 Slippers, B., Crous, P. W., Jami, F., Groenewald, J. Z., and Wingfield, M. J. 2017. Diversity in
578 the Botryosphaeriales: Looking back, looking forward. Fungal Biol. 121:307-321.
579 Smith, H., Wingfeld, M, J., Coutinho, T. A., and Crous, P. W. 1996. *Sphaeropsis sapinea* and
580 *Botryosphaeria dothidea* endophytic in *Pinus* spp. and *Eucalyptus* spp. in South Africa.
581 S. Afr. J. Bot. 62:86-88.
582 Spadaro, D., Meloni, G.R., Siciliano, I., Prencipe, S., and Gullino, M.L. 2020. HPLC-MS/MS
583 method for the detection of selected toxic metabolites produced by *Penicillium* spp. in
584 nuts. Toxins 12: 307.
585 Swofford, D. L. 2003. PAUP* Phylogenetic Analysis Using Parsimony, (*and Other Methods);
586 Version 4.0 b10; Sinauer Associates: Sunderland, MA, USA.
587 Teviotdale, L., Michailides, T. J., and Pscheidt, J. W. 2002. Compendium of Nut Crop Diseases
588 in Temperate Zones. American Phytopathological Society, St Paul, MN, USA, pp 100.
589 Thambugala KM, Daranagama DA, Phillips AJL, Bulgakov TS et al. 2017 – Microfungi on
590 Tamarix. Fungal Diversity 82:239–306.
591 Thompson, S. M., Tan, Y. P., Young, A. J., Neate, S. M., Aitken, E. A. B., and Shivas, R. G.
592 2011. Stem cankers on sunflower Helianthus annuus in Australia reveal a complex of
593 pathogenic *Diaporthe* (Phomopsis) species. Persoonia 27:80–89.
594 Udayanga, D., Castlebury, L. A., Rossman, A. Y., Chukeatirote, E., and Hyde, K. D. 2015. The
595 *Diaporthe sojae* species complex: phylogenetic re-assessment of pathogens associated
596 with soybean, cucurbits and other field crops. Fungal. Biol. 119:383-407.
597 Udayanga, D., Castlebury, L. A., Rossman, A. Y., Chukeatirote, E., and Hyde, K. D. 2014.
598 Insights into the genus *Diaporthe*: phylogenetic species delimitation in the *D. eres*
599 species complex. Fungal Diversity 67:203-229.

600 Udayanga, D., Liu, X., Crous, P. W., McKenzie, E. H. C., Chukeatirote, E., and Hyde, K. D.
601 2012. A multi-locus phylogenetic evaluation of *Diaporthe* (Phomopsis). Fungal Diversity
602 56:157-171.
603 Udayanga, D., Liu, X., McKenzie, E. H., Chukeatirote, E., Bahkali, A. H., and Hyde, K. D.
604 2011. The genus Phomopsis: biology, applications, species concepts and names of
605 common phytopathogens. Fungal Diversity 50:189-225.
606 Valente, S., Meloni, G.R., Prencipe, S., Spigolon, N., Somenzi, M., Fontana, M., Gullino, M.L.,
607 and Spadaro, D. 2020. Effect of drying temperature and exposure times on *Aspergillus*
608 *flavus* growth and aflatoxin production on artificially inoculated hazelnuts. J. Food Prot.
609 83:1241-1247.
610 Vitale, S. M., Scarpari, L., Luongo, M., Galli, A., Belisario, G., Schreiber, M., Petrucci, G.,
611 Fontaniello, T., De Gregorio, G., Castello. 2020. Nocciola avariata, un fenomeno in
612 aumento che abbatte la qualità**.** Rivista di Frutticoltura, published online (available at:
613 https://rivistafrutticoltura.edagricole.it/post-raccolta/nocciola-avariata-un-fenomeno-in-
614 aumento-che-abbatte-la-qualita/)
615 Waqas, M., Guarnaccia, V., and Spadaro, D. 2022. First Report of Nut Rot Caused by
616 *Neofusicoccum parvum* on Hazelnut (Corylus avellana) in Italy. Plant Dis. 106:1987.
617 Wehmeyer, L. E. 1926. A biologic and phylogenetic study of stromatic Sphaeriales. Am. J. Bot.
618 13:575-645.
619 White. T. J., Bruns, T., Lee, S., and Taylor, J. 1990. Amplification and direct sequencing of
620 fungal ribosomal RNA genes for phylogenetics. In: PCR Protocols: a guide to methods
621 and applications. (Innis MA, Gelfand DH, Sninsky JJ, White TJ, eds). Academic Press,
622 New York, USA. 315–322.

623 Wiman, N. G., Webber III, J. B., Wiseman, M., and Merlet, L. 2019. Identity and pathogenicity
624 of some fungi associated with hazelnut (Corylus avellana L.) trunk cankers in Oregon.
625 Plos one 14:e0223500.
626 Yang, Q., Fan, X. L., Guarnaccia, V., and Tian, C. M. 2018. High diversity of *Diaporthe* species
627 associated with twelve new species described. MycoKeys 39:97-149.
628 Yang, Q., Jiang, N., and Tian, C. M. 2020. Three new *Diaporthe* species from Shaanxi province,
629 China. MycoKeys 67:1.
630 Yang, Q., Jiang, N., and Tian, C. M. 2020. Three new *Diaporthe* species from Shaanxi province,
631 China. MycoKeys, 67:1.
632 Yang, Q., Jiang, N., and Tian, C. M. 2021. New species and records of Diaporthe from Jiangxi
633 Province, China. MycoKeys, 77:41.

Zapata, M., Palma, M. A., Aninat, M. J., and Piontelli, E. 2020. Polyphasic studies of new species of *Diaporthe* from native forest in Chile, with descriptions of *Diaporthe araucanorum* sp. nov., *Diaporthe foikelaweni* sp. nov. and *Diaporthe patagonica* sp. nov. Int. J. Syst. Evol. Microbiol. 70:3379-3390.

Tables

Table 1: Overall incidence of all *Diaporthe* spp. on hazelnut nuts (*Corylus avellana*) variety and date of cultivation from different towns in Piedmont, Italy

Sr. No.	**Towns/Province [1]**	**Variety [2]**	**Date of orchard planting [3]**	***Diaporthe* incidence (%)**
1	Lu and Cuccaro (AL)	TGP	NA	30.43
2	Murazzano (CN)	TGP	2010	82
3	Marsaglia (CN)	TGP	1995	63.6
4	Rodello (CN)	TGP	1990	47
5	Cravanzana (CN)	TGP	1995	36.3
6	Cortemilia (CN)	TGP	1980	50
7	Borgo D'Ale (VC)	TGP	2011	8.3
8	Cavaglià (BI)	TGP	2013	42.4
9	Belvedere Langhe (CN)	TGP	1975	32

[1] Provinces are administrative areas in Italy: AL (Alessandria); CN (Cuneo); BI (Biella); VC (Vercelli).

[2] TGP: 'Tonda Gentile del Piemonte'

[3] NA: not available

Figures

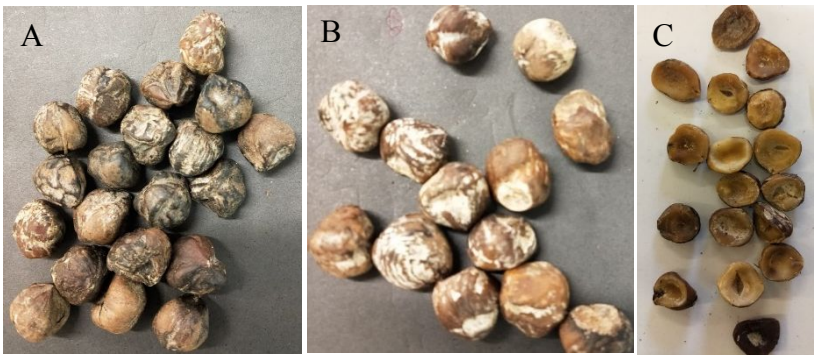

Fig. 1. Symptoms observed on hazelnut (*Corylus avellana*) described as (A) black rot (B) moldy (C) necrotic.

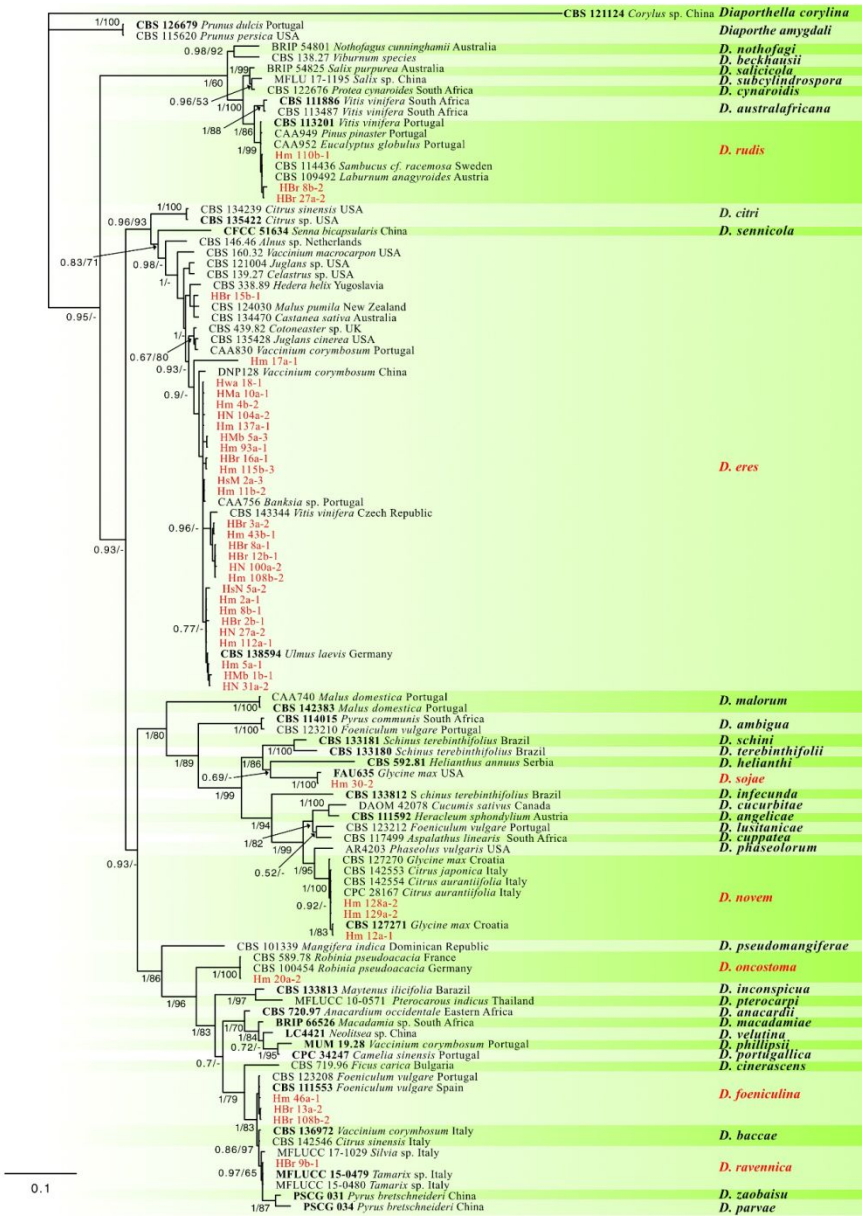

Fig. 2. Consensus phylogram of 2,622 trees resulting from a Bayesian analysis of the combined ITS, *tef-1α*, and *tub2* sequence alignments of the *Diaporthe* species. Bootstrap support values and Bayesian posterior probability values are indicated at the nodes. Host and country of origin are listed next to the strain numbers. Ex-type isolates are indicated in bold. The isolates obtained in this study are in red. The tree was rooted with *Diaporthella corylina* (CBS 121124).

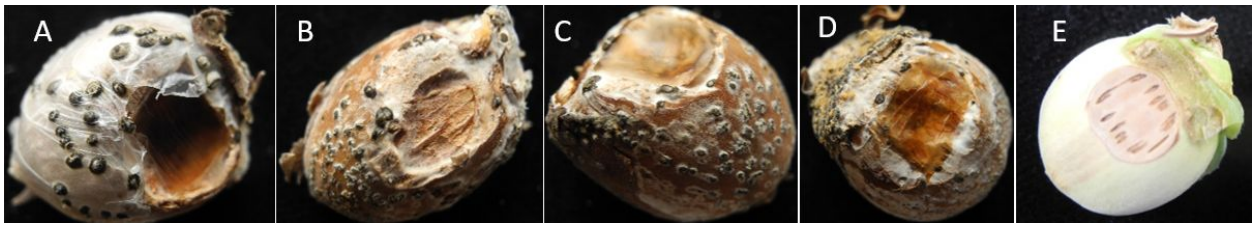

Fig. 3. Symptomatology induced on hazelnut nuts 'Tonda Gentile del Piemonte' inoculated with *Diaporthe* spp. and stored at 22±2 °C for 30 days in a chamber with a 12 h light/12 h dark. Symptoms of nut rot were evaluated by the following scale: 0: no visible symptoms (**E**); 1: <25% development of pycnidia (**D**); 2: 25-50% development of pycnidia (**C**); 3: 50-75% development of pycnidia (**B**); 4: ≥75% development of pycnidia (**A**).

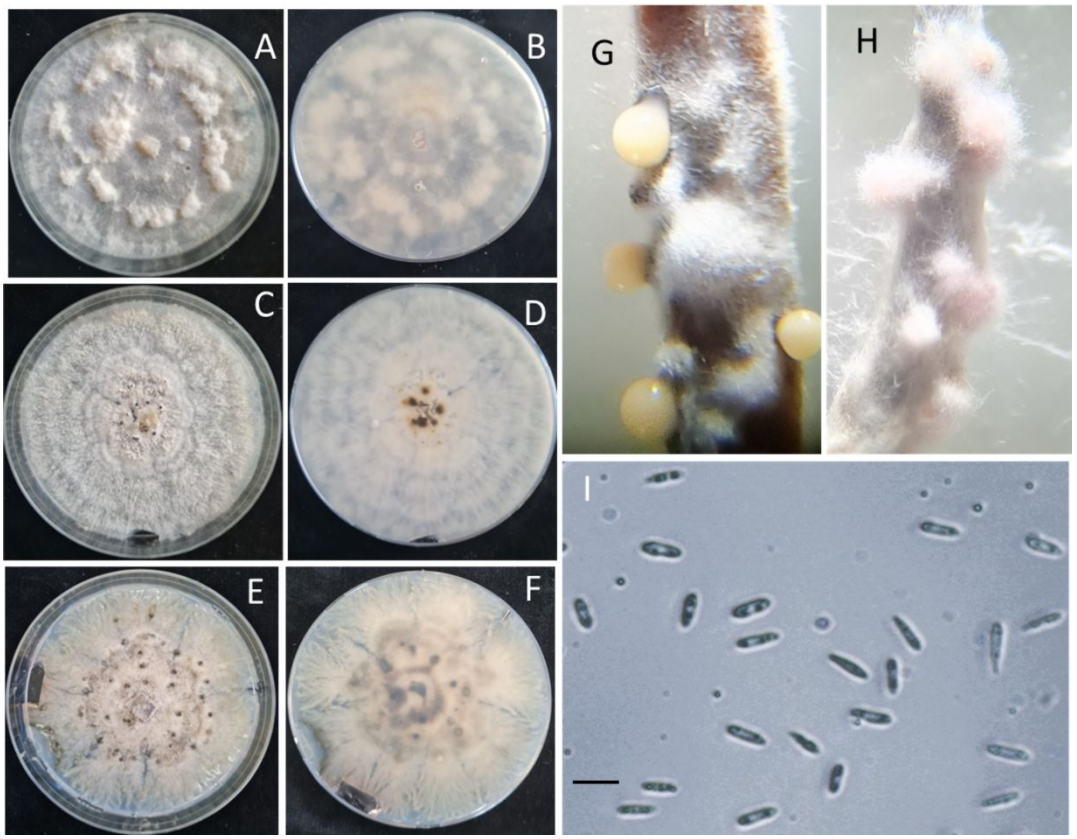

Fig. 4 Morphological features of *Diaporthe* spp. obtained from hazelnut nuts. **(A-B)** *D. sojae*. Front and reverse side of colony grown on PDA after 10 days at 23 ± 2 °C**(C-D)** *D. ravennica*. Front and reverse side of colony grown on PDA **(E-F)** *D. eres*. Front and reverse side of colony grown on PDA after 10 days at 23 ± 2 °C. (**G)** Conidiomata of *D. eres* on sterilized pine needle on WA. (**H**) Conidiomata of *D. sojae* on sterilized pine needle on WA **(I)** Conidia of *D. eres* (dimensions: 8.5-11.1x 3.5-4.5 µm; scale bar: 10 µm).

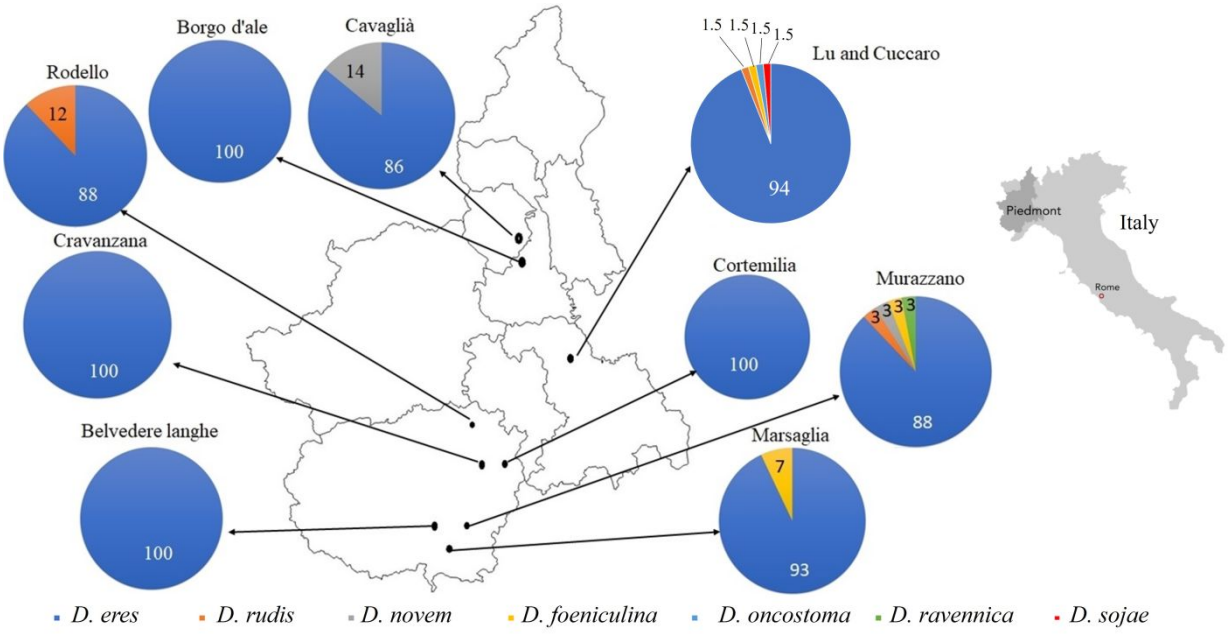

Fig. 5. Incidence (%) and distribution of *Diaporthe* species from hazelnut nuts (*Corylus avellana*) according to their sampling locations of Piedmont, Italy.

e-Xtra (Supplementary) Files

Table S1.

Isolates of *Diaporthe* spp. across nine regions of Piedmont, Italy, obtained from hazelnut (*Corylus avellana*) during 2020-2021 and their GenBank accession numbers.

Sr. no.	Isolate code	Fungal species	Isolation year	Towns/Provinces[1]	Altitude	GenBank Accession [2]		
						ITS	*tef1-α*	*tub2*
1	Hwa-18-1	*Diaporthe eres*	2020	Lu and Cuccaro (AL)	307 m	OM331706	ON933990	OP186258
2	HsN5a-2	*D. eres*	2020	Lu and Cuccaro (AL)	307 m	OM331707	ON933991	OP186259
3	HsM2a-3	*D. eres*	2020	Lu and Cuccaro (AL)	307 m	OM331708	ON933992	OP186260
4	HMb-1b-1	*D. eres*	2020	Lu and Cuccaro (AL)	307 m	OM331709	ON933993	-
5	HMb-5a-3	*D. eres*	2020	Lu and Cuccaro (AL)	307 m	OM331710	ON933994	OP186261
6	Hma-10a-1	*D. eres*	2020	Lu and Cuccaro (AL)	307 m	OM331711	ON933995	OP186262
7	HM-2a-1	*D. eres*	2020	Murazzano (CN)	739 m	OM331712	ON933996	OP186263
8	HM-4b-2	*D. eres*	2020	Murazzano (CN)	739 m	OM331713	ON933997	OP186264
9	HM-5a-1	*D. eres*	2020	Murazzano (CN)	739 m	OM331714	ON933998	OP186265
10	HM-8b-1	*D. eres*	2020	Murazzano (CN)	739 m	OM331715	ON933999	OP186266
11	HM-11b-2	*D. eres*	2020	Murazzano (CN)	739 m	OM331716	ON934000	OP186267
12	Hm-12a-1	*D. novem*	2020	Murazzano (CN)	739 m	OM331738	ON933987	OP156876
13	HM-17a-1	*D. eres*	2020	Murazzano (CN)	739 m	OM331717	ON934001	OP186268
14	Hm-20a-2	*D. oncostoma*	2020	Murazzano (CN)	739 m	ON911324	ON934002	OP186269
15	HBR-2b-1	*D. eres*	2020	Murazzano (CN)	739 m	OM331718	OP288105	OP186270
16	HBr-3a-2	*D. eres*	2020	Murazzano (CN)	739 m	ON911327	OP296410	OP186271
17	HBR-8a-1	*D. eres*	2020	Murazzano (CN)	739 m	OM331719	ON934003	OP186272
18	HBr-8b-2	*D. rudis*	2020	Murazzano (CN)	739 m	OM331733	ON934004	OP186273
19	HBr-9b-1	*D. ravennica*	2020	Murazzano (CN)	739 m	ON911325	ON934005	OP186274
20	HBR-12b-1	*D. eres*	2020	Murazzano (CN)	739 m	OM331720	ON934006	OP186275
21	HBr-13a-2	*D. foeniculina*	2020	Murazzano (CN)	739 m	ON911322	ON934007	OP186276

22	HBR-15b-1	*D. eres*	2020	Murazzano (CN)	739 m	OM331721	ON934008	OP186277
23	HBR-16a-1	*D. eres*	2020	Murazzano (CN)	739 m	OM331722	ON934009	OP186278
24	HN-27a-2	*D. eres*	2021	Lu and Cuccaro (AL)	307 m	OM331723	ON934010	OP186279
25	HBr-27a-2	*D. rudis*	2021	Lu and Cuccaro (AL)	307 m	OM331734	ON934011	OP186280
26	Hm-30-2	*D. sojae*	2021	Lu and Cuccaro (AL)	307 m	ON911326	ON934012	OP186281
27	HN-31a-2	*D. eres*	2021	Lu and Cuccaro (AL)	307 m	OM331724	ON934013	OP186282
28	HM-43b-1	*D. eres*	2021	Lu and Cuccaro (AL)	307 m	OM331725	ON934014	OP186283
29	Hm-46a-1	*D. foeniculina*	2021	Lu and Cuccaro (AL)	307 m	ON911323	ON934015	-
30	HM-93a-1	*D. eres*	2021	Cortemilia (CN)	247 m	OM331726	ON934016	OP186284
31	HN-100a-2	*D. eres*	2021	Cravanzana (CN)	580 m	OM331727	ON934017	OP186285
32	HM-108b-2	*D. eres*	2021	Marsaglia (CN)	550 m	OM331728	ON934018	OP186286
33	HN-104a-2	*D. eres*	2021	Belvedere Langhe (CN)	679 m	OM331729	ON934019	OP186287
34	Hm-110b-1	*D. rudis*	2021	Rodello (CN)	600 m	OM331735	ON934020	OP186288
35	HM-112a-1	*D. eres*	2021	Rodello (CN)	600 m	OM331730	ON934021	OP186289
36	HM-115b-3	*D. eres*	2021	Rodello (CN)	600 m	OM331731	ON934022	OP186290
37	Hm-128a-2	*D. novem*	2021	Cavaglià (BI)	270 m	OM331737	ON933988	OP156877
38	Hm-129a-2	*D. novem*	2021	Cavaglià (BI)	270 m	OM331736	ON933989	OP156878
39	HBr-108b-2	*D. foeniculina*	2021	Cavaglià (BI)	270 m	ON911321	ON934023	OP186291
40	HM-137a-1	*D. eres*	2021	Borgo D'Ale (VC)	240 m	OM331732	-	OP186292

[1] AL: Alessandria, CN: Cuneo, BI: Biella, VC: Vercelli; [2] ITS: internal transcribed spacers 1 and 4 together with 5.8S nrDNA; *tef1-α*: translation elongation factor 1-α gene; *tub2*: beta-tubulin gene. Sequences generated in this study indicated in italics.

Table S2.

List of reference sequences of *Diaporthe* spp. including the outgroup *Diaporthella corylina* used in phylogenetic analyses for this study. Information includes GenBank accession numbers, strains, host, and origins.

Species	Strain [1]	Host	Country	GenBank Accession [2]		
				ITS	*tef1-α*	*tub2*
Diaporthe ambigua	CBS 114015^{T}	*Pyrus communis*	South Africa	KC343010	KC343736	KC343978
D. ambigua	CBS 123210	*Foeniculum vulgare*	Portugal	KC343012	KC343738	KC343980
D. amygdali	CBS 126679^{T}	*Prunus dulcis*	Portugal	KC343022	KC343748	KC343990
D. amygdali	CBS 115620	*Prunus persica*	USA	KC343020	KC343746	KC343988
D. anacardii	CBS 720.97^{T}	*Anacardium occidentale*	Eastern Africa	KC343024	KC343750	KC343992
D. angelicae	CBS 111592^{T}	*Heracleum sphondylium*	Austria	KC343027	KC343753	KC343995
D. australafricana	CBS 111886	*Vitis vinifera*	South Africa	KC343038	KC343764	KC344006
D. australafricana	CBS 113487^{T}	*Vitis vinifera*	South Africa	KC343039	KC343765	KC344007
D. baccae	CBS 136972^{T}	*Vaccinium corymbosum*	Italy	KJ160565	KJ160597	MF418509
D. baccae	CBS 142546	*Citrus sinensis*	Italy	MF418358	MF418437	MF418517
D. beckhausii	CBS 138.27	*Viburnum species*	Unknown	KC343041	KC343767	KC344009
D. citri	CBS 134239	*Citrus cinensis*	USA	KC357553	KC357522	KC357456
D. citri	CBS 135422^{T}	*Citrus* sp.	USA	KC843311	KC843071	KC843187
D. cinerascens	CBS 719.96	*Ficus carica*	Bulgaria	KC343050	KC343776	KC344018
D. cucurbitae	DAOM 42078	*Cucumis sativus*	Canada	KM453210	KM453211	KP118848
D. cuppatea	CBS 117499	*Aspalathus linearis*	South Africa	KC343057	KC343783	KC344025
D. cynaroidis	CBS 122676	*Protea cynaroides*	South Africa	KC343058	KC343784	KC344026
D. eres	CBS 138594^{T}	*Ulmus laevis*	Germany	KJ210529	KJ210550	KJ420799
D. eres	CBS 143344	*Vitis vinifera*	Czech Republic	MG281020	MG281541	MG281193
D. eres	CAA756	*Banksia* sp.	Portugal	MW040531	MW052385	MW091320
D. eres	CBS 146.46	*Alnus* sp.	The Netherlands	KC343008	KC343734	KC343976
D. eres	CBS 121004	*Juglans* sp.	USA	KC343134	KC343860	KC344102

D. eres	CBS 124030	*Malus pumila*	New Zealand	KC343149	KC343875	KC344117
D. eres	CBS 134470	*Castanea sativa*	Australia	KC343146	KC343872	KC344114
D. eres	DNP128	*Vaccinium corymbosum*	China	KC763096	KJ210561	KJ420801
D. eres	CBS 139.27	*Celastrus* sp.	USA	KC343047	KC343773	KC344015
D. eres	CBS 135428	*Juglans cinerea*	USA	KC843328	KC843121	KC843229
D. eres	CBS 439.82	*Cotoneaster* sp.	UK	KC343090	KC343816	KC344058
D. eres	CBS 338.89	*Hedera helix*	Yugoslavia	KC343152	KC343878	KC344120
D. eres	CBS 160.32	*Vaccinium macrocarpon*	USA	AF317578	GQ250326	KC344196
D. eres	MUM 19.31=CAA830	*Vaccinium corymbosum*	Portugal	MK792309	MK828080	MK837931
D. foeniculina	CBS 123208	*Foeniculum vulgare*	Portugal	KC343104	KC343830	KC344072
D. foeniculina	CBS 111553^{T}	*Foeniculum vulgare*	Spain	KC343101	KC343827	KC344069
D. helianthi	CBS 592.81^{T}	*Helianthus annuus*	Serbia	KC343115	KC343841	KC344083
D. inconspicua	CBS 133813^{T}	*Maytenus ilicifolia*	Brazil	KC343123	KC343849	KC344091
D. infecunda	CBS 133812^{T}	*Schinus terebinthifolius*	Brazil	KC343126	KC343852	KC344094
D. lusitanicae	CBS 123212	*Foeniculum vulgare*	Portugal	KC343136	KC343862	KC344104
D. macadamiae	BRIP 66526^{T}	*Macadamia* sp.	South Africa	MN708230	MN696528	MN696539
D. malorum	CAA740	*Malus domestica*	Portugal	KY435642	KY435629	KY435670
D. malorum	CBS 142383^{T}	*Malus domestica*	Portugal	KY435638	KY435627	KY435668
D. nothofagi	BRIP 54801	*Nothofagus cunninghamii*	Australia	JX862530	JX862536	KF170922
D. novem	CBS 127270	*Glycine max*	Croatia	KC343156	KC343882	KC344124
D. novem	CBS 127271^{T}	*Glycine max*	Croatia	KC343157	KC343883	KC344125
D. novem	CPC 26188 =CBS 142553	*Citrus japonica*	Italy	MF418426	MF418505	MF418586
D. novem	CPC 28165 = CBS 142554	*glycine max*	Italy	MF418427	MF418506	MF418587
D. novem	CPC 28167	*Citrus aurantiifolia*	Italy	MF418428	MF418507	MF418588
D. oncostoma	CBS 589.78	*Robinia pseudoacacia*	France	KC343162	KC343888	KC344130
D. oncostoma	CBS 100454	*Robinia pseudoacacia*	Germany	KC343160	KC343886	KC344128
D. parvae	PSCG 034^{T}	*Pyrus bretschneideri*	China	MK626919	MK654858	MK691248
D. phaseolorum	CBS 139281=AR4203	*Phaseolus vulgaris*	USA	KJ590738	KJ590739	KJ610893

D. phillipsii	MUM 19.28^{T}	*Vaccinium corymbosum*	Portugal	MK792305	MK828076	MN000351
D. portugallica	CBS 144228=CPC34247^{T}	*Camelia sinensis*	Portugal	MH063905	MH063911	MH063917
D. pseudomangiferae	CBS 101339= MFLU 15-3228^{T}	*Mangifera indica*	Dominican Republic	KC343181	KC343907	KC344149
D. pterocarpi	MFLUCC 10-0571	*Pterocarous indicus*	Thailand	JQ619899	JX275416	JX275460
D. ravennica	MFLUCC 17-1029	*Salvia* sp.	Italy	KY964191	KY964147	KY964075
D. ravennica	MFLUCC 15-0479^{T}	*Tamarix* sp.	Italy	KU900335	KX365197	KX432254
D. ravennica	MFLUCC 15-0480	*Tamarix* sp.	Italy	KU900336	KX426703	KX377688
D. rudis	CBS 114436	*Sambucus cf. racemosa*	Sweden	KC343236	KC343962	KC344204
D. rudis	CBS 109492	*Laburnum anagyroides*	Austria	KC343232	KC343958	KC344200
D. rudis	CBS 113201^{T}	*Vitis vinifera*	Portugal	KC343234	KC343960	KC344202
D. rudis	CAA949	*Pinus pinaster*	Portugal	MN190304	MT309426	MT309452
D. rudis	CAA952	*Eucalyptus globulus*	Portugal	MN190307	MT309429	MT309455
D. salicicola	BRIP 54825	*Salix purpurea*	Australia	JX862531	JX862537	KF170923
D. schini	CBS 133181T	*Schinus terebinthifolius*	Brazil	KC343191	KC343917	KC344159
D. sennicola	CFCC 51634	*Senna bicapsularis*	China	KY203722	KY228883	KY228889
D. sojae	CBS 139282=FAU635^{T}	*Glycine max*	USA	KJ590719	KJ590762	KJ610875
D. subcylindrospora	MFLU 17-1195	*Salix* sp.	China	MG746629	MG746630	MG746631
D. terebinthifolii	CBS 133180^{T}	*Schinus terebinthifolius*	Brazil	KC343216	KC343942	KC344184
D. velutina	CGMCC 3.18286=LC4421^{T}	*Neolitsea* sp.	China	KX986790	KX999182	KX999223
D. zaobaisu	PSCG031^{T}	*Pyrus bretschneideri*	China	MK626922	MK654855	MK691245
Diaporthella corylina	CBS 121124^{T}	*Corylus* sp.	China	KC343004	KC343730	KC343972

[1] BRIP: Plant Pathology Herbarium, Department of Primary Industries, Dutton Park, Queensland, Australia CAA: Culture Collection Artur Alves, University of Aveiro, Aveiro, Portugal; CBS: Westerdijk Fungal Biodiversity Institute, Utrecht, The Netherlands; CFCC: China Forestry Culture Collection Center, Beijing, China; CGMCC: China, General Microbiological Culture Collection, Beijing, China; CMW: Forestry and Agricultural Biotechnology Institute, University of Pretoria, South Africa; CPC: Culture collection of P.W. Crous, housed at Westerdijk Fungal Biodiversity Institute; DAOMC: The Canadian Collection of Fungal Cultures, Canada; DNP: Isolates in SMML culture collection, USDA-ARS, Beltsville, USA; FAU: Isolates in culture collection of Systematic Mycology and Microbiology Laboratory, USDA-ARS, Beltsville, MD, USA; LC: Working

collection of Lei Cai,housed at Institute of Microbiology, Chinese; MFLU: Herbarium of Mae Fah Luang University, Thailand; MIFCC: Michigan Isolate Fungal Culture Collection, Michigan, USA; MUM: Culture Collection from Micoteca da Universidade do Minho, Center for Biological Engineering of University of Minho, Braga, Portugal. Ex-type isolates are indicated with ^{T}.

[2] ITS: internal transcribed spacers 1 and 4 together with 5.8S nrDNA; *tef1-α*: translation elongation factor 1-α gene; *tub2*: beta-tubulin gene. Sequences generated in this study indicated in italics.

Table S3. Pathogenicity test of *Diaporthe* spp. on hazelnut nuts (*Corylus avellana*) and their disease severity

Sr. no.	Isolates code	Fungal spp.	DS% [1]	SD [2]	TK [3]
1	Hwa-18-1	*Diaporthe eres*	86.1	4.81	efg
2	HsN5a-2	*D. eres*	80.6	9.62	defg
3	HsM2a-3	*D. eres*	77.8	4.81	defg
4	HMb-1b-1	*D. eres*	83.3	8.33	efg
5	HMb-5a-3	*D. eres*	100.0	0.00	g
6	Hma-10a-1	*D. eres*	80.6	4.81	defg
7	HM-2a-1	*D. eres*	75.0	8.33	cdefg
8	HM-4b-2	*D. eres*	91.7	8.33	fg
9	HM-5a-1	*D. eres*	80.6	9.62	defg
10	HM-8b-1	*D. eres*	83.3	8.33	efg
11	HM-11b-2	*D. eres*	88.9	9.62	efg
12	Hm-12a-1	*D. novem*	77.8	9.62	defg
13	HM-17a-1	*D. eres*	97.2	4.81	fg
14	Hm-20a-2	*D. oncostoma*	36.1	4.81	abcd
15	HBR-2b-1	*D. eres*	52.8	4.81	bcdef
16	HBr-3a-2	*D. eres*	55.6	9.62	bcdefg
17	HBR-8a-1	*D. eres*	86.1	9.62	efg
18	HBr-8b-2	*D. rudis*	86.1	4.81	efg
19	HBr-9b-1	*D. ravennica*	13.9	9.62	ab
20	HBR-12b-1	*D. eres*	88.9	12.73	efg
21	HBr-13a-2	*D. foeniculina*	72.2	4.81	cdefg
22	HBR-15b-1	*D. eres*	88.9	9.62	efg
23	HBR-16a-1	*D. eres*	58.3	8.33	bcdefg
24	HN-27a-2	*D. eres*	86.1	9.62	efg
25	HBr-27a-2	*D. rudis*	13.9	4.81	ab
26	Hm-30-2	*D. sojae*	91.7	8.33	fg
27	HN-31a-2	*D. eres*	69.4	12.73	cdefg
28	HM-43b-1	*D. eres*	88.9	12.73	efg
29	Hm-46a-1	*D. foeniculina*	77.8	12.73	defg
30	HM-93a-1	*D. eres*	94.4	4.81	fg
31	HN-100a-2	*D. eres*	58.3	8.33	bcdefg
32	HM-108b-2	*D. eres*	58.3	8.33	bcdefg
33	HN-104a-2	*D. eres*	80.6	4.81	defg
34	Hm-110b-1	*D. rudis*	94.4	4.81	fg
35	HM-112a-1	*D. eres*	44.4	9.62	abcde
36	HM-115b-3	*D. eres*	86.1	12.73	efg
37	Hm-128a-2	*D. novem*	30.6	4.81	abc
38	Hm-129a-2	*D. novem*	75.0	0.00	cdefg
39	HBr-108b-2	*D. foeniculina*	100.0	0.00	g
40	HM-137a-1	*D. eres*	75.0	0.00	cdefg
41	Healthy Control		0.00	0.00	a

[1] Disease severity in percentage [2] standard deviation [3] Tukey test

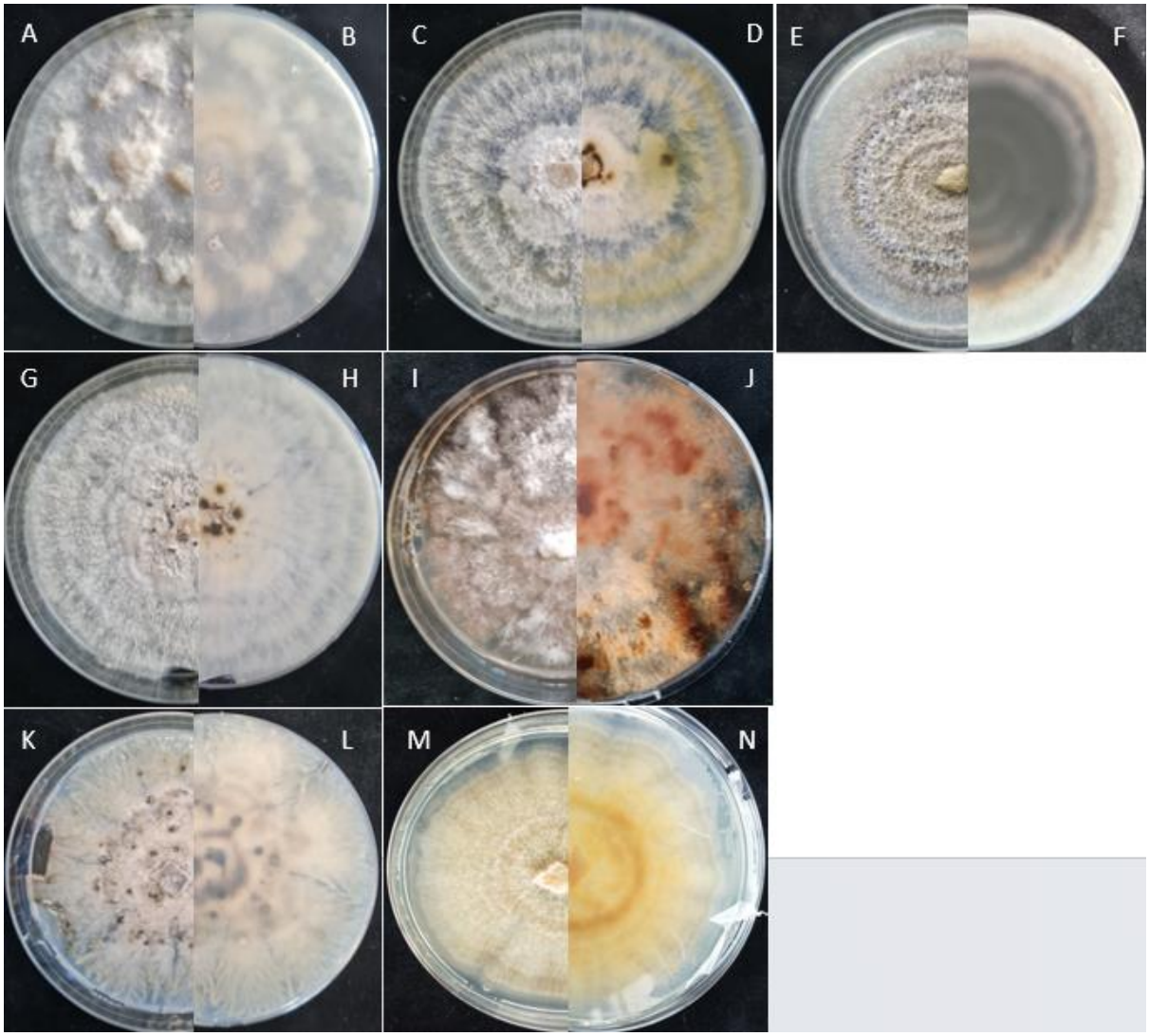

Fig. S1. Macromorphology of *Diaporthe* spp. obtained from hazelnut nuts **(A-B)** *D. sojae*. Front and reverse side of colony grown on PDA after 10 days at 23 ± 2 °C, **(C-D)** *D. foeniculina*. Front and reverse side of colony grown on PDA after 10 days at 23 ± 2 °C, **(E-F)** *D. novem*. Front and reverse side of colony grown on PDA after 10 days at 23 ± 2 °C, (**G-H)** *D. ravennica*. Front and reverse side of colony grown on PDA at 23 ± 2 °C, (**I-J)** *D. rudis*. Front and reverse side of colony grown on PDA after 10 days at 23 ± 2 °C, **(K-L)** *D. eres*. Front and reverse side of colony grown on PDA after 10 days at 23 ± 2 °C, (**M-N)** *D. oncostoma*. Front and reverse side of colony grown on PDA after 10 days at 23 ± 2 °C.

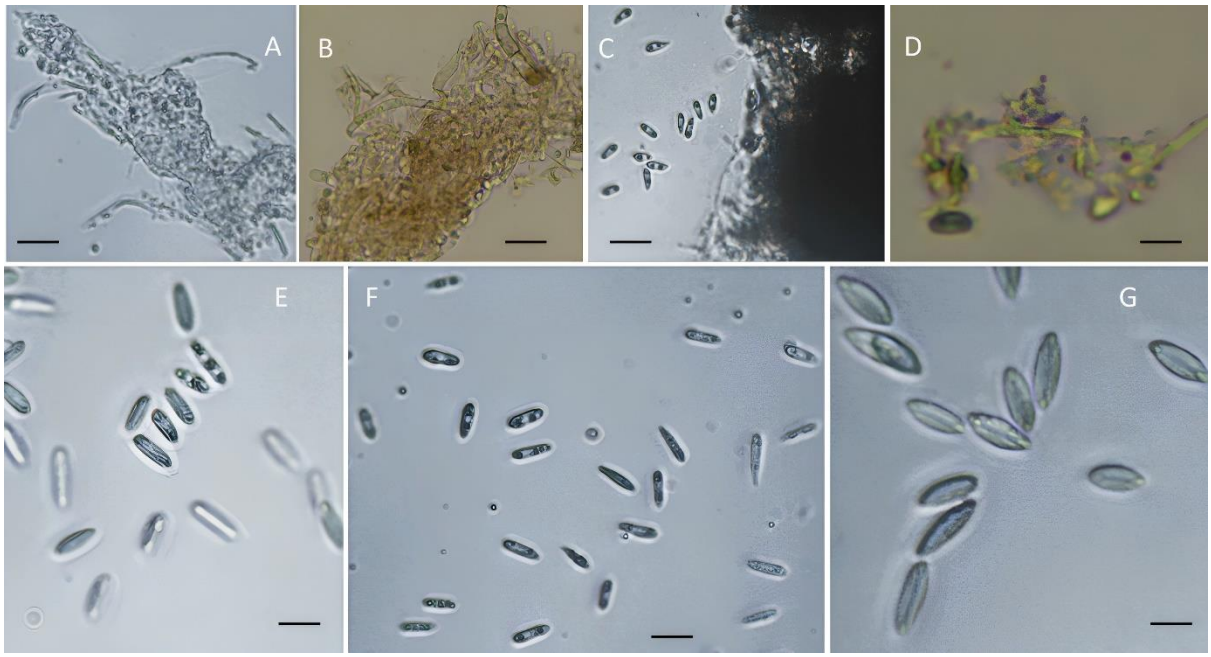

Fig. S2. Micromorphological features of *Diaporthe* spp. obtained from hazelnut nuts **(A)** Conidia of *D. sojae* (dimensions 5.8-7.3x2-3.2; scale bar: 10 µm), **(B)** Conidia of *D. foeniculina* (dimensions 7.6-9.5x2.5-2.9 µm; scale bar: 10 µm), **(C)** Conidia of *D. novem* (dimensions: 6.9-9.1x2.5-2.9 µm; scale bar: 10 µm), **(D)** Conidia of *D. ravennica* (dimensions 8.3-11.9x2.5-4.3 µm; scale bar: 10 µm), **(E)** Conidia of *D. rudis* (dimensions: 7.5-8.5x2.4-2.7 µm; scale bar: 10 µm), **(F)** Conidia of *D. eres* (dimensions: 8.5-11.1x 3.5-4.5 µm; scale bar: 10 µm), **(G)** Conidia of *D. oncostoma* (11-14.5x 3.2-4.9 µm; scale bar: 10 µm).